

Prediction of Γ -L and L-X crossovers in $\text{Ga}_x\text{Al}_{1-x}\text{Sb}$ alloys by empirical pseudopotential method

Nishant N. Patel and K.B. Joshi^a

Department of Physics, ML Sukhadia University, Udaipur-313001, India

Received 18 April 2007 / Received in final form 22 August 2007

Published online 5 October 2007 – © EDP Sciences, Società Italiana di Fisica, Springer-Verlag 2007

Abstract. Using empirical pseudopotential method Γ -L crossover is found for the $\text{Ga}_{0.74}\text{Al}_{0.26}\text{Sb}$. The conduction band minimum is observed to switch at the (0.87, 0, 0) point for $\text{Ga}_{0.51}\text{Al}_{0.49}\text{Sb}$ which shifts to the X point for $\text{Ga}_{0.21}\text{Al}_{0.79}\text{Sb}$ and remains at X leading finally to indirect band gap in AlSb. Band structure calculations for a large number of alloys are performed and bowing parameters b_X and b_L are proposed for the E_X and E_L respectively. Our findings may serve as directive to select the materials in a range of composition to examine the bowing parameters and thereby effective mass experimentally for the $\text{Ga}_x\text{Al}_{1-x}\text{Sb}$ alloys.

PACS. 71.15.Dx Computational methodology – 71.20.-b Electron density of states and band structure of crystalline solids – 71.22.+i Electronic structure of liquid metals and semiconductors and their alloys – 71.55.Eq III-V semiconductors

1 Introduction

The III-V ternary semiconductor alloys are receiving increasing attention due to the optoelectronic properties within the window of wavelength 1.3–1.6 μm [1]. The $\text{Ga}_x\text{Al}_{1-x}\text{Sb}$ heterostructures have been identified as quantum well infrared photo-detectors [2]. The interplay of direct band gap in GaSb and indirect band gap in AlSb as well as inter-subband transitions in these random alloys are of high importance to propose promising materials for the cutting edge technological applications in detectors and lasers [3]. The applications can be identified by determining the band structure which guides to tailor materials of required band gap at various symmetry points. Despite direct and indirect band gap measurements reported on the $\text{Ga}_x\text{Al}_{1-x}\text{Sb}$ alloys, many ambiguities are remaining in the concentration dependence of Γ -L and Γ -X band gaps and the bowing parameters due to limited number of compositions studied. Noticeably, a few Greene semiconducting alloys [4] and ternary III-V alloys [5] have been studied by empirical tight binding method. For the III-V semiconducting alloys of our interest in this work, the empirical bands reported [5,6] are calculated from less accurate form factors and do not predict the nature of band gaps correctly for compounds like AlSb [6]. Thus, the materials have not been studied rigorously with this view point using empirical pseudopotential method (EPM) [7], $\mathbf{k}\cdot\mathbf{p}$ [8] method or the quasiparticle scheme [9]. However, all these methods can be applied as a directive to

unfold ambiguities in the concentration dependent band gaps and related quantities. Local density approximation (LDA) based methods underestimate [10] the band gaps and hence can not be applied.

EPM, a highly reliable and rapidly converging method, is applicable to semiconducting compounds and alloys. Recently the effect of lattice mismatch on the band structure of III-V semiconducting alloys has been studied employing improved virtual crystal approximation (VCA) [11]. It has been observed that the improved VCA gives better results for alloys having larger lattice mismatch than the simple VCA whereas simple VCA works equally well for alloys having smaller lattice mismatch. The lattice mismatch is very small for GaAlAs and GaAlSb alloys. Consequently, disorder effects are expected to play less significant role in determining the electronic structure of these alloys compared to the InAsP, GaAsSb and InPSb [11,12]. In this work, therefore, the EPM under simple VCA has been applied to calculate band structures of $\text{Ga}_x\text{Al}_{1-x}\text{Sb}$ alloys [11] considering the zinc-blende structures.

2 Method of computation

In EPM [7] the crystal potential $V(\mathbf{r})$ is generated by superposition of atomic potentials, which involves fitting of atomic form factors to the experimental data:

$$V(\mathbf{r}) = \sum_{R,\tau} V_a(\mathbf{r} - \mathbf{R} - \boldsymbol{\tau}) \quad (1)$$

^a e-mail: k_joshi@yahoo.com

here, the summation extends over the lattice vectors \mathbf{R} , basis vectors $\boldsymbol{\tau}$, and the number of atoms in the primitive cell. In real space the crystal potential can be written as:

$$V(\mathbf{r}) = \sum_{\mathbf{G}} V_a(\mathbf{G}) S(\mathbf{G}) e^{i\mathbf{G}\cdot\mathbf{r}} \quad (2)$$

where $V_a(\mathbf{G})$ is the form factor for the atomic potential and $S(\mathbf{G})$ is the structure factor. The structure factor $S(\mathbf{G})$ is given by:

$$S(\mathbf{G}) = (1/N_a) \sum_{\boldsymbol{\tau}} e^{-i\mathbf{G}\cdot\boldsymbol{\tau}} \quad (3)$$

here N_a is the number of basis atoms. For zinc-blende structures if the origin is taken halfway between the two FCC structures then $\boldsymbol{\tau} = \pm(\frac{1}{8}, \frac{1}{8}, \frac{1}{8})a$ and for $A^N B^{8-N}$ compounds like AlSb and GaSb the crystal potential in reciprocal space can be simplified as:

$$V(\mathbf{G}) = V^S(\mathbf{G}) \cos(\mathbf{G} \cdot \boldsymbol{\tau}) + iV^A(\mathbf{G}) \sin(\mathbf{G} \cdot \boldsymbol{\tau}) \quad (4)$$

$$\text{where } V^S(\mathbf{G}) = \frac{1}{2} [V_A(\mathbf{G}) + V_B(\mathbf{G})] \quad \text{and}$$

$$V^A(\mathbf{G}) = \frac{1}{2} [V_A(\mathbf{G}) - V_B(\mathbf{G})] \quad \text{and}$$

$V^S(\mathbf{G})$ and $V^A(\mathbf{G})$ are the symmetric and antisymmetric form factors respectively. The pseudo wavefunction $\Psi_{n,k}(\mathbf{r})$ is a solution of the Schrodinger equation with the potential $V(\mathbf{r})$. In the local EPM [7] the $\Psi_{n,k}(\mathbf{r})$ is expanded in plane wave basis set as:

$$\Psi_{n,k}(\mathbf{r}) = \sqrt{\frac{1}{\Omega}} \sum_{\mathbf{G}} C_{n,k}(\mathbf{G}) e^{i(\mathbf{k}+\mathbf{G})\cdot\mathbf{r}} \quad (5)$$

where $C_{n,k}(\mathbf{G})$ is the coefficient of the plane wave for a given reciprocal vector \mathbf{G} and Ω is the volume of the unit cell.

As mentioned earlier, due to very small lattice mismatch the simple VCA works well for the $\text{Ga}_x\text{Al}_{1-x}\text{Sb}$ alloys [11]. Moreover, unlike metallic alloys the approximation has been observed to work reasonably well to examine band gaps, effective masses in other III-V and II-VI ternary and multi-component semiconductor alloys [13,14]. Therefore the simple VCA within the EPM has been applied to compute band structure. To determine the band structure, 350 plane waves were considered and the potential was generated from the parameters proposed by Zaoui et al. [15] without spin-orbit effects. The convergence in the charge density and energy was ensured with the accuracy of 1 part in 10^5 . Total accumulation of charge in the charge density computation was confirmed regarding accuracy of the scheme [16]. The calculations are performed for $\text{Ga}_x\text{Al}_{1-x}\text{Sb}$ alloys with ($0 \leq x \leq 1$ in steps of 0.2). The lattice constants for the alloys were derived from Vegards' law [17] which gives accurate results particularly for III-V semiconducting alloys [18].

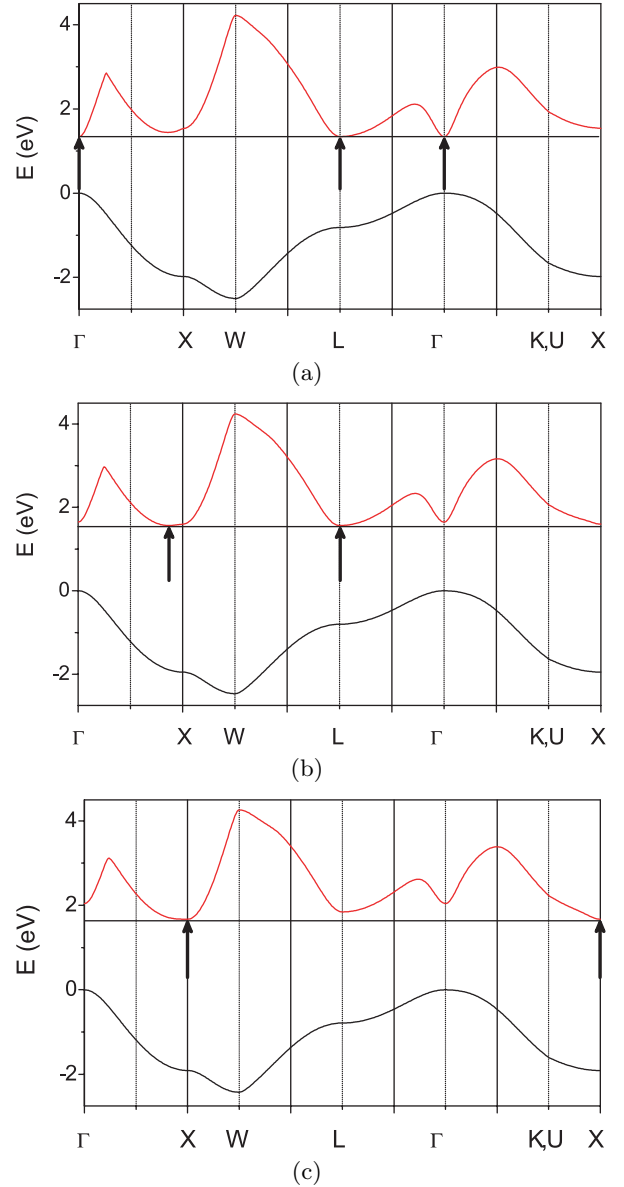


Fig. 1. (a). The first conduction band and the top valence band for $\text{Ga}_{0.74}\text{Al}_{0.26}\text{Sb}$ alloy. All the energies are measured with reference to the top valence band at Γ . The arrows indicate the positions of conduction band minimum. (b) The first conduction band and the top valence band for $\text{Ga}_{0.51}\text{Al}_{0.49}\text{Sb}$ alloy. (c) The first conduction band and the top valence band for $\text{Ga}_{0.21}\text{Al}_{0.79}\text{Sb}$ alloy.

3 Results and discussions

The evolution of band structures for a few $\text{Ga}_x\text{Al}_{1-x}\text{Sb}$ alloys covering the first conduction band and the top valence band is shown in Figure 1. Figures 1a–1c show the band structures for only a few compositions which are important with specific reference to the crossovers and shifting in the conduction band minimum (CBM) along $\Gamma \rightarrow \text{L} \rightarrow \text{X}$. The EPM band structure of GaSb shows the direct band gap at Γ . On increasing the content of Al the conduction

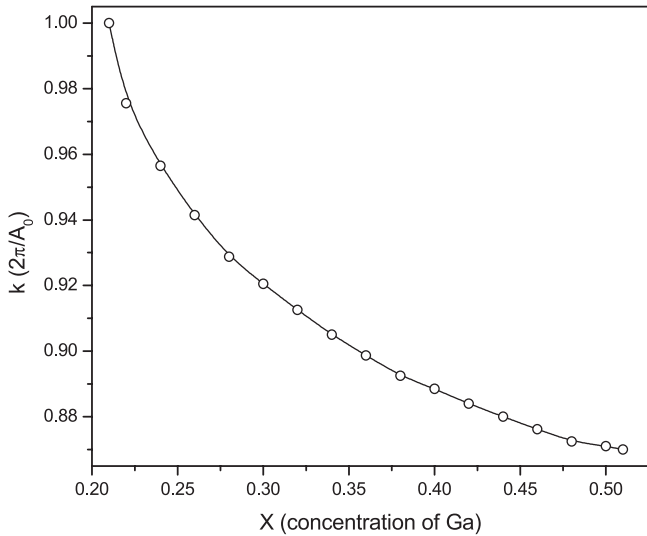


Fig. 2. Shift of the k -points from $(0.87, 0, 0)$ to $(1, 0, 0)$ showing conduction band minimum with concentration x ($0.21 \leq x \leq 0.51$) of Ga.

band minimum remains at Γ and a crossover to L point for $\text{Ga}_{0.74}\text{Al}_{0.26}\text{Sb}$ alloy is found as shown by arrows in Figure 1a. This closely resembles with the highly resolved and reliable experimental data reported by Bignazzi et al. [19] who observed this crossover at $x = 0.78$. From Figure 1b it is obvious that on increasing the content of Al further, the CBM remains at L and another crossover is found at $(0.87, 0, 0)$ for $\text{Ga}_{0.51}\text{Al}_{0.49}\text{Sb}$. This is in contrast to the exact crossover at X as reported experimentally by Alibert and co-workers [20]. With increase in the content of Al further, the CBM starts to shift towards the X-point as shown in Figure 1c.

Now we discuss the shift of conduction band minimum with composition of alloys in the ($0.21 \leq x \leq 0.52$) range. In Figure 2 we have plotted the k -points giving CBM versus gallium concentration (x) in the alloys in this specific range. Figure 2 depicts that the CBM shows non-linear shift on decreasing the concentration of gallium and finally settles at X point for $\text{Ga}_{0.21}\text{Al}_{0.79}\text{Sb}$. Thereafter the minimum remains at X upto AlSb. These results are compared in Table 1 and the crossovers are graphically presented in Figure 3. Table 1 also includes the compositions showing exact crossover experimentally. The Γ -L crossover proposed by our EPM calculation is in good agreement with both the experiments however it is closer to the experiment of Bignazzi et al. [19] who employed the experimental artefacts and the standard data reduction techniques. It is clear that the L-X crossover reported for $\text{Ga}_{0.52}\text{Al}_{0.48}\text{Sb}$ by Alibert et al. [20] is in good accordance with the composition proposed by our work whereas Bignazzi et al. [19] did not study the compositions wherein the L-X crossover takes place.

With regard to L-X crossover, it is worthwhile to note that Alibert et al. [20] studied the alloys in the range ($0.0 \leq x \leq 0.48$) and graphically predicted the conduc-

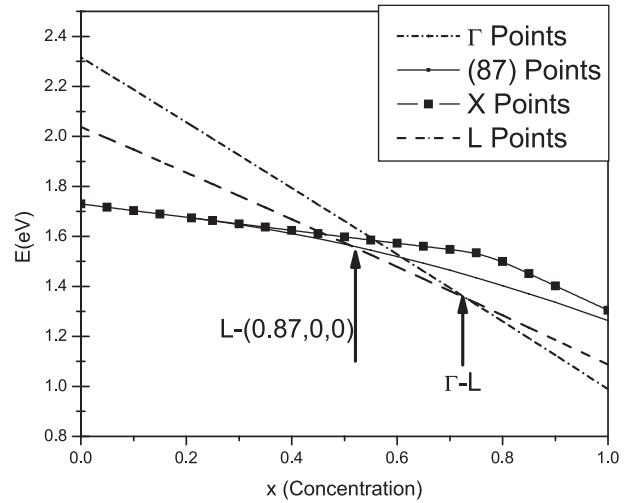


Fig. 3. The variation of E_X , E_Γ and E_L with composition x for the $\text{Ga}_x\text{Al}_{1-x}\text{Sb}$ alloys. The two crossovers $L-(0.87, 0, 0)$ and Γ -L are marked by arrows. The solid line (—) represents conduction band energies between the points $(0.86, 0, 0)$ to X $(1, 0, 0)$. After the second crossover the minima shifts from $(0.87, 0, 0)$ to X $(1, 0, 0)$ and the solid line merges with the line of X points at higher concentrations of Al.

tion band minimum to occur for the $\text{Ga}_{0.52}\text{Al}_{0.48}\text{Sb}$ alloy at the symmetry point X. Our calculation clearly indicates (Fig. 2) that CBM switches at the point $(0.87, 0, 0)$ for $x = 0.51$ and moves along the direction $(0.87, 0, 0) \rightarrow X$ with Al content which settles finally at the point X for $\text{Ga}_{0.21}\text{Al}_{0.79}\text{Sb}$. The range (i.e. $0.0 \leq x \leq 0.51$) is also important for device applications. To get more relevant experimental information in this range, one requires to study large number of alloys in this range experimentally. Our findings may serve as directive to select the samples within a limited range ($0.0 \leq x \leq 0.51$) to observe the indirect band gap which will be highly useful in addressing the uncertainties in the bowing parameter at E_X experimentally.

Bowing parameters b_Γ , b_L and b_X deduced from our band structure calculations together with the available experimental and theoretical results are summarised in Table 2. To determine the bowing parameter b_X from our calculations, we have plotted variation of E_X (i.e. CBM in the neighbourhood of X point) with x ($0.0 \leq x \leq 0.51$) in Figure 4 and fitted a quadratic polynomial suggesting bowing parameter $C = (-0.23)$. Column IV of Table 2 shows that it deviates from the recommended zero bowing [21]. It is noticeable that to examine the bowing b_X at E_X one must consider the compositions showing conduction band minimum in the neighbourhood of X rather than the entire range as done in the experimental study of bowing parameters [20,21]. This could be the reason for disagreement of recommended experimental value with our proposed value. To determine the bowing parameter b_L the best fit was found for a quadratic polynomial and b_L is found to be -0.04 , close to the recommended zero value [19,21] shown in Column III of Table 2. We find it

Table 1. The range of compositions (x) of $\text{Ga}_x\text{Al}_{1-x}\text{Sb}$ alloys showing the minimum in the first conduction band at the Γ , L and X symmetry points. The quantities in the parentheses show the exact crossover composition proposed.

	Γ	L	X
Alibert et al. [20]	1–0.84 (0.84)	0.84–0.52 (0.52)	0.52–0.0
Bignazzi et al. [19]	1–0.78 (0.78)	0.78–0.59	—
This work	1–0.74 (0.74)	0.74–0.51 (0.51)	0.51–0.0 [†]

[†]For 0.51–0.21 the conduction band minimum shift is $[(0.87, 0, 0) \rightarrow \text{X}]$ whereas for 0.21–0.0 it is at $[\text{X}]$.

Table 2. The bowing parameters of $\text{Ga}_x\text{Al}_{1-x}\text{Sb}$ alloys.

		b_Γ	b_L	b_X
Alibert et al. [20]		0.48	0.55	0.0
Bignazzi et al. [19]		0.00	0.00	—
Vurgaftman et al. [21]		$-0.044 + 1.22x$	0.00	0.00
Bechiri et al. [11]	With disorder	0.47	.26	0.15
	Without disorder	-0.02	-0.17	-0.01
This work		0.00	-0.04	-0.23

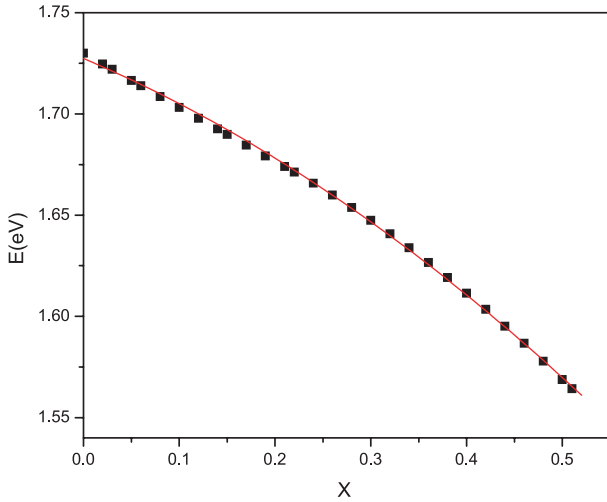


Fig. 4. Plot of energy E_X with composition x in the range ($0.0 \leq x \leq 0.51$) for $\text{Ga}_x\text{Al}_{1-x}\text{Sb}$ alloys. E_X is the energy of the conduction band minimum in the neighbourhood of X $[(0.87, 0, 0) \text{ to } (1, 0, 0)]$ with reference to the top valence band at Γ . The fitted polynomial is $E_X = 1.727 - (0.199)x - (0.231)x^2$ (eV).

worth to mention that the χ^2 was $\sim 10^{-12}$ and 10^{-8} for the quadratic and linear fits respectively suggesting non-linear character albeit of very small magnitude.

From Tables 1 and 2 one can infer that the predictions of crossovers and bowing parameters derived from our calculations are in good agreement with the highly reliable experimental data [19]. Moreover, our calculations show better agreement with measurement compared to the calculations of Bechiri et al. [11] which considers disorder effects also. To examine the disorder effects more critically measurements on a number of alloys in the proposed range of compositions shall be highly useful.

4 Conclusions

On the basis of simple VCA within the EPM, the conduction band minimum at the L point has been observed in the range ($0.51 \leq x \leq 0.74$) for the $\text{Ga}_x\text{Al}_{1-x}\text{Sb}$ alloys. Our results are well in accordance with the range proposed by the experiments. The agreement of the b_L bowing parameter could be attributed to the correctly selected range of materials [19] undertaken in the experimental investigations. This affirms our assertion that to find bowing, one needs to consider only those compositions which show minimum at the point of interest. The accord between theory and experiment also supports the findings of Bechiri et al. [11] that the simple VCA sufficiently accounts for the electronic structure and related quantities for semiconductor alloys having very small lattice mismatch. For more rigorous comparison reflection high-energy electron diffraction (RHEED) and high-resolution X-ray diffraction (HRXRD) measurements on selected range of materials shall be highly fruitful. It is hoped that our work may stimulate experimental investigations along these lines.

This work is supported by the Department of Science and Technology, New Delhi through grant No. SR/S2/CMP-15/2004.

References

1. H. Xie, W.I. Wang, Appl. Phys. Lett. **63**, 776 (1993)
2. B.F. Levine, J. Appl. Phys. **74**, 1(R) (1993)
3. A.G. Milnes, A.Y. Polyakov, Solid-State Electron. **36**, 803 (1993)
4. D.W. Jenkins, K.E. Newman, J.D. Dow, Phys. Rev. B **32**, 4034 (1985)
5. A.-B. Chen, A. Sher, Phys. Rev. B **22**, 3886 (1980)

6. M.L. Cohen, T.K. Bergstresser, Phys. Rev. **141**, 789 (1966)
7. M.L. Cohen, J.R. Chelikowsky, in *Electronic structure and optical properties of Semiconductors*, edited by M. Cordona (Springer, Berlin, 1988), Vol. 75
8. F. Bassani, G.P. Parravicini, in *Electronic States and Optical Transitions in Solids*, edited by R.A. Ballinger (Pergamon, New York, 1975)
9. A. Rubio, J.L. Corkill, M.L. Cohen, E.L. Shirley, S.G. Louie, Phys. Rev. B **48**, 11810 (1993)
10. M.S. Hybertsen, S.G. Louie, Phys. Rev. Lett. **55**, 1418 (1985)
11. A. Bechiri, F. Benmakhlouf, N. Bouarissa, Mater. Chem. Phys. **77**, 507 (2003)
12. J.A. Van Vechten, T.K. Bergstresser, Phys. Rev. B **1**, 3351 (1970)
13. N. Bouarissa, Eur. Phys. J. B **32**, 421 (2003)
14. F. Long, P. Harrison, W.E. Hagston, J. Appl. Phys. **79**, 6939 (1996)
15. A. Zaoui, M. Ferhat, B. Khelifa, J.P. Dufour, H. Aourag, Phys. Stat. Sol. (b) **185**, 163 (1994)
16. K.B. Joshi, Nishant N. Patel, To appear in Pramana – J. of Phys. (2007)
17. L. Vegard, Z. Phys. **5**, 17 (1921)
18. Z. Dridi, B. Bouhafs, P. Ruterana, Semiconductor Sci. Technol. **108**, 850 (2003)
19. A. Bignazzi, E. Grilli, M. Guzzi, C. Bocchi, A. Bosacchi, S. Franchi, R. Magnanini, Phys. Rev. B **57**, 2295 (1998)
20. C. Alibert, A. Joullie, A.M. Joullie, C. Ance, Phys. Rev. B **27**, 4946 (1983)
21. I. Vurgaftman, J.R. Meyer, L.R. Ram-Mohan, J. Appl. Phys. **89**, 5815 (2001)